Available online at www.sciencedirect.com
SCIENCE DIRECT
Cement and Concrete Research 36 (2006) 716 – 722
Cement and Concrete Research

Thaumasite formation in a tunnel of Bapanxia Dam in Western China

Baoguo Ma [a], Xiaojian Gao [a,*], Ewan A. Byars [b], Qizhi Zhou [c]

[a] Key Laboratory of Silicate Materials Science and Engineering of Ministry of Education, Wuhan University of Technology, Wuhan 430070, China
[b] CMRU, Department of Civil and Structural Engineering, University of Sheffield, Mappin Street, Sheffield S1 3JD, UK
[c] Department of Engineering Materials, University of Sheffield, Mappin Street, Sheffield S1 3JD, UK

Received 17 December 2004; accepted 9 October 2005

Abstract

A site investigation and sampling was carried out on a sulfate-attacked concrete structure in Bapanxia Hydraulic Power Plant in Western China. The concrete had been exposed to ground water containing substantial concentrations of salts (SO_4^{2-}, CO_3^{2-} and Cl^-) for about 6 years and was analyzed with X-ray diffraction (XRD), scanning electron microscopy (SEM), energy dispersive X-ray spectroscopy (EDX), laser-Raman spectroscopy and Fourier transform infrared (FTIR) spectroscopy. It is shown that a white mushy mixture consisting of thaumasite, ettringite, gypsum and calcite is present in the residual concrete. This paper reports the first instance of the thaumasite form of sulfate attack of concrete in China.

Keywords: Concrete (E); Thaumasite; Sulfate attack (C); Carbonation (C)

1. Introduction

Thaumasite is a naturally occurring mineral of the type $Ca_6[Si(OH)_6]_2(CO_3)_2(SO_4)_2{\cdot}24H_2O$, which has been found in metamorphosed rocks that have undergone hydrothermal changes over time [1]. Erlin and Stark [2] first reported its occurrence in concrete construction in sanitary sewer pipes and at the base of a core taken from an 11-year-old pavement. Since then, the thaumasite form of sulfate attack (TSA) has caused varying degrees of deterioration within a wide variety of cementitious building systems [3], the most notable of these being the 1998 discovery of TSA causing severe deterioration of the buried concrete foundations of several bridges on the M5 motorway in England [4]. As a result, the UK Government convened the Thaumasite Expert Group (TEG) and a report dealing with thaumasite sulfate attack was issued in 1999 [5]. Consequently, TSA has become recognized as a separate form of sulfate attack and has been found in different buildings of England, US, Canada, France, Switzerland, Germany, Norway and other places [3,6,7].

The preconditions for TSA [3,8] are (i) contact with sulfate solution, (ii) the presence of CO_3^{2-} from limestone-dust-filler in cement, limestone- and dolomite-aggregate in concrete, from carbonation of concrete or even from the environment [9], (iii) the presence of SiO_3^{2-}, mainly from CSH, the main OPC hydration phase. Lower temperatures (lower than 15 °C) can also favour the thaumasite formation and TSA attack. Notwithstanding the need for carbonate, these conditions would also be expected to lead to ettringite ($Ca_6[Al(OH)_6]_2(SO_4)_3{\cdot}26H_2O$) formation, which has been reported as the main product of sulfate attack [10]. Due to the similarity of XRD patterns of thaumasite and ettringite, it is quite likely that at least some previously reported cases of sulfate attack that were attributed to ettringite formation may have been TSA.

This paper presents a series of observations of field elements of the Bapanxia Hydraulic Power Plant on the Yellow River in Northwestern China, which is severely affected by sulfate attack. The attacked concrete was analyzed to identify the deterioration products and reaction mechanisms. X-ray powder diffraction (XRD), scanning electron microscopy (SEM) coupled with energy dispersive X-ray spectroscopy (EDX), laser-Raman

Table 1
Composition of the water sample (mg/l)

$K^+ + Na^+$	Ca^{2+}	Mg^{2+}	Cl^-	SO_4^{2-}	HCO_3^-
12893	1026	524	17801	6638	223

* Corresponding author. Tel.: +86 27 62416862.
E-mail address: xjgao2002@yahoo.com.cn (X. Gao).

0008-8846/$ - see front matter © 2005 Elsevier Ltd. All rights reserved.
doi:10.1016/j.cemconres.2005.10.011

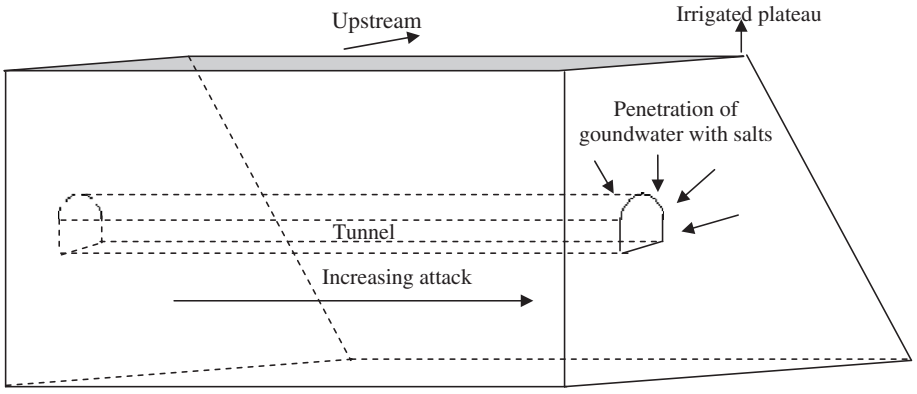

Fig. 1. Schematic diagram showing the concrete dam layout.

spectroscopy and Fourier transform infrared (FTIR) spectroscopy test methods were used.

2. Site investigation

Bapanxia Hydraulic Power Plant is located on the Yellow River in Xigu District of Lanzhou City, China and was constructed between 1969 and 1975. The area is mountainous, with undulating bedrock covered by silty aeolin deposits known as loess [11]. These bedrocks are orange-red sandstones and tan-red mudstones, the upper portion of which is gypsiferous [12]. Sandstone is of relatively low permeability [13], which results in the permeating water flowing slowly and dissolving a mass of soluble salts during the pervasion. This results in the groundwater typically containing significant amounts of sulfate, chloride and a substantial mass of carbonate. A sample of the groundwater from the northern side of the dam (the most severely attacked) was analyzed and the result is shown in Table 1.

Fig. 1 shows the general layout of the dam, looking upstream. The irrigated plateau is situated on the north bank of the dam along the river, where the soil and the groundwater contain a high concentration of sulfate. Observations within the tunnel suggest that the run-off water, which is rich in sulfate, percolates from the outer surface through cracks and preformed ducts to reach the tunnel, where it collects in the drainage channel. At the points of entry, the tunnel wall concrete is also seriously attacked, particularly at the northern end which is closer to the irrigated plateau. In some areas, deep deposits of white crystalline salts were also seen deposited on the tunnel walls, confirming the flow of mineralized water through the concrete into the tunnel.

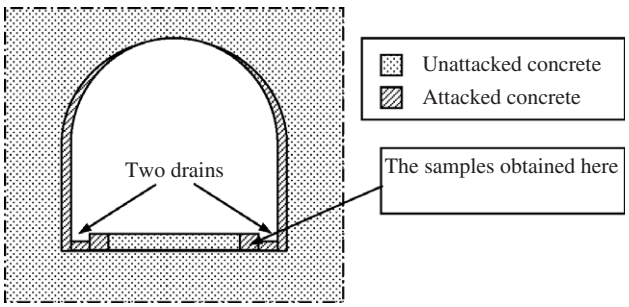

Fig. 2. Schematic illustration of the tunnel and areas most affected by TSA.

Fig. 2 shows a cross-section of the tunnel in the dam and highlights specific areas where damage has been observed. The damage is predominantly in the drainage channels but is also observed on the walls and roof in localities where the water enters the tunnel. The deepest effects appear to penetrate to around 100 mm from the surface. However, a full core analysis is recommended to determine the actual depth and type of attack observed at greater depths.

Fig. 3 shows a general view across the dam to the mountain, from where the aggressive salts originate. The lighter-coloured areas above the dam in Fig. 3 are, in fact, sulfate salt deposits on the surface of the soil. Consequently, the water penetrating the tunnel has enough sulfates (Table 1) to cause severe sulfate attack and is equivalent to a Class DS-5 sulfate solution [14]. Within the tunnel, temperatures range between 4 and 10 °C with a continuous relative humidity of more than 85%. Additionally, carbonated concrete in the tunnel, dissolved CO_2 in the water and dissolved carbonates in the water would appear to be a likely source of CO_3^{2-}. Thus, conditions favourable to TSA are present.

The northern side tunnel is the most severely damaged by sulfate attack and has been repaired every few years since the dam was constructed. The last restoration was in 1997, when all the damaged surface concrete was replaced with a high-quality cement concrete made with ordinary Portland cement and a

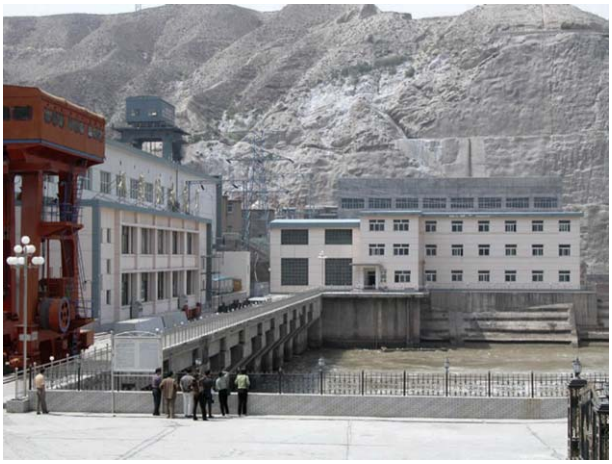

Fig. 3. Profile of Bapanxia Hydraulic Power Plant.

Fig. 4. Deterioration in the tunnel drainage channels.

natural gravel coarse aggregate with a maximum size of 10 mm. In 2004, most of the floor and wall concrete appeared to be undamaged, but there was very severe deterioration along edges of the drainage channels at either side (Fig. 4). Here, the concrete shows expansion, cracking and softening in some regions with the maximum depth of damage being more than 100 mm. Some of the concrete lost its strength completely and could be easily crumbled by hand, in which case the cement paste transformed into a white, pulpy mass with no strength. These are very typical symptoms of TSA [4,6] and these samples were retained for further analysis.

3. Experimental methods

Samples of the soft crumbly degraded concrete from the site were carefully chosen and preserved for laboratory investigations, and only one typical sample was analyzed. After a macroscopic examination of sections through the whole region of interest, the white, pulpy substance was prepared for analysis by X-ray diffraction (XRD), scanning electron microscopy (SEM), energy dispersive X-ray spectroscopy (EDX), laser-Raman spectroscopy and Fourier transform infrared (FTIR) spectroscopy. These tests are capable of identifying thaumasite and other attack products.

XRD patterns were collected on an automated Japan D/MAX-IIIA X-ray diffractometer operating at 35 kV and 30 mA using CuK_α radiation. Data was collected between 5° and 60° 2θ using a step-size of 0.02° and a count time of 0.6 s per step.

A JEOL SX-4 scanning electron microscope (SEM) was used and the accelerating voltage was maintained at 20 kV. Samples were coated with a thin film of gold before testing. The elemental micro-analyses of samples were identified by an energy dispersive X-ray spectroscopy (EDX) coupled with the SEM system. The resolution power of EDX is 129.92 eV and the testing time is set to 50 s.

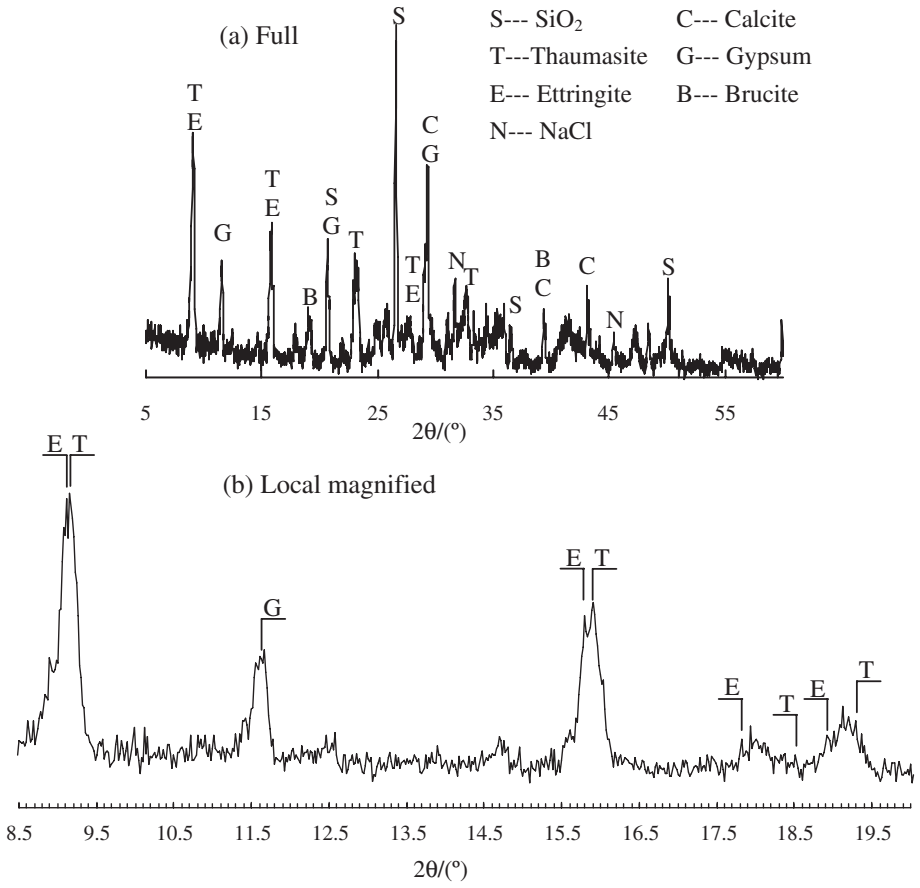

Fig. 5. XRD pattern of the eroded concrete sample.

Raman spectroscopic measurements were carried out using a Renishaw Raman Microprobe (Type RM-1000), with a laser (514.5 nm) excitation source having a power at the specimen of the order of 2.5 mW. The Charge Coupled Device (CCD) exposure time was 30 s and every sample scanned 10 times. Raman spectra data were generated from 200 cm^{-1} to 1500 cm^{-1} in 2 cm^{-1} increments.

Fourier transform infrared (FTIR) spectroscopy was carried out using a Nicolet 60 SXB FTIR Spectrophotometer. Samples were prepared for analysis by grinding a known mass of solid with dried KBr. The resulting powder was then pressed at 2000 psi for 5 min to produce a pellet for analysis. The wavenumber ranges analysed were from 400 cm^{-1} to 4000 cm^{-1}.

4. Results and discussion

4.1. XRD analysis

The XRD analysis result is shown in Fig. 5(a), where it can be seen that, due to the deterioration, there is little trace of the products of normal cement hydration such as portlandite (CH) in the XRD trace. The trace indicates that several crystalline phases exist in the sample, these being thaumasite ($Ca_6[Si(OH)_6]_2(CO_3)_2(SO_4)_2{\cdot}24H_2O$), ettringite ($Ca_6[Al(OH)_6]_2(SO_4)_3{\cdot}26H_2O$), gypsum ($CaSO_4{\cdot}2H_2O$), calcite ($CaCO_3$), some brucite ($Mg(OH)_2$), quartz and a little sodium chloride (NaCl). The XRD patterns of thaumasite and ettringite are similar [15], but both of them were recognized when the XRD pattern was locally magnified in Fig. 5(b). Gypsum, another detected product of sulfate attack is present in the trace as is calcite, which is formed from the carbonation of portlandite. Brucite is formed from the attack of dissolved Mg^{2+} on portlandite. It is thought that the sodium chloride (NaCl) has been precipitated from dissolved NaCl in the groundwater [16].

4.2. SEM–EDX testing

Fig. 6 shows SEM images of the mushy sample at two resolutions. Fig. 6(a) shows that no CH crystal exists in the sample, and this compound is needed to preserve the integrity of CSH. Many club-shaped or needle crystals embedded irregularly in the pulpy material with a very open microstructure. Under higher magnification (Fig. 6(b)), a large number of needle crystals up to 0.5 μm in diameter and 3–4 μm in length, predominantly with parallel orientation and with smooth and even surfaces can be seen. The appearance of these crystals is very similar to thaumasite as described in Ref. [17]. An EDX of this crystal is shown in Fig. 7 and indicates the presence of calcium, silicon, sulfur, aluminum, carbon, oxygen and some of chlorine and sodium. A higher Si and lower Al peak indicates that these needle crystals are predominantly thaumasite with a small quantity of ettringite.

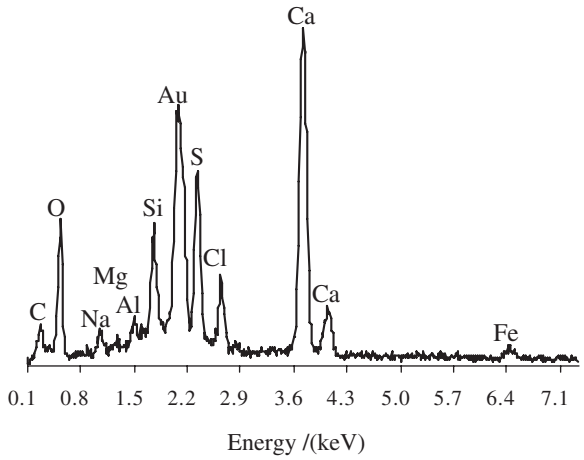

Fig. 7. EDX spectrum of the needle-like crystal in the square zone of Fig. 6(b).

4.3. Raman spectrum

The Raman spectrum for the deteriorated concrete sample is shown in Fig. 8. The literature [18] indicates that:

i) thaumasite has three major peaks at 658 cm^{-1}, 990 cm^{-1}, and 1076 cm^{-1} corresponding to Si–OH, sulfate and carbonate groups, respectively, and three minor peaks at 417 cm^{-1}, 453 cm^{-1}, and 479 cm^{-1} may be also observed;

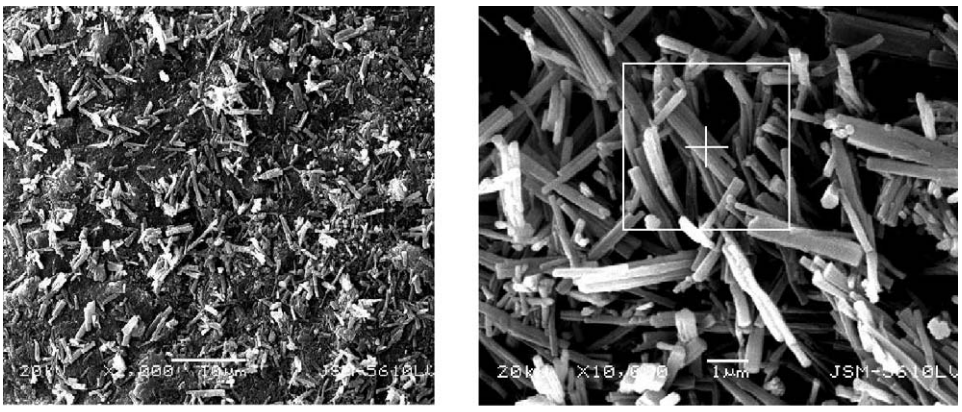

(a) Some club-shaped crystals in the sludge (b) Needle-like crystals in the same sample

Fig. 6. SEM photos of the deteriorated concrete mush from Bapanxia Hydraulic Station.

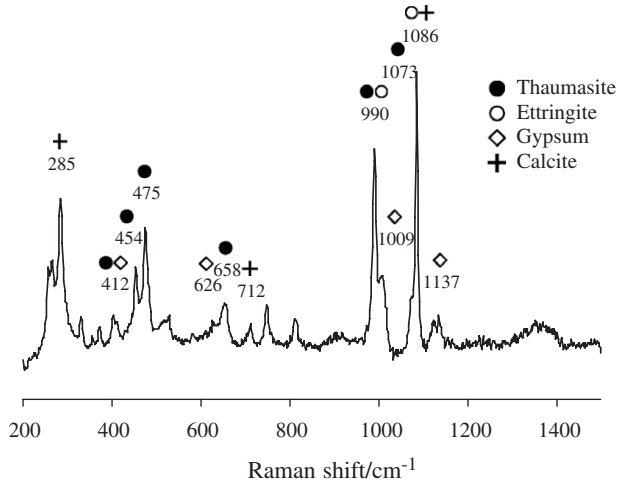

Fig. 8. Raman spectrum of the deteriorated concrete.

ii) ettringite has two major peaks at 990 cm^{-1} and 1088 cm^{-1} and three minor peaks at 449 cm^{-1}, 548 cm^{-1}, 617 cm^{-1}, respectively;
iii) gypsum has one major peak at 1009 cm^{-1} and five minor peaks at 417 cm^{-1}, 496 cm^{-1}, 621 cm^{-1}, 673 cm^{-1} and 1137 cm^{-1};
iv) three peaks at 1086 cm^{-1}, 713 cm^{-1} and 285 cm^{-1} exist in the calcite Raman spectrum pattern [19].

The strongest peaks at 990 cm^{-1} and 1076 cm^{-1} for thaumasite are assigned to sulfate and carbonate groups, respectively. The first peak is similar to the characteristic peak at 990 cm^{-1} for ettringite and the second one is close to the strongest peak at 1086 cm^{-1} for calcite and another strong peak at 1088 cm^{-1} for ettringite. Therefore, it is difficult to distinguish thaumasite from ettringite and calcite based on these two strongest peaks alone. However, thaumasite has a special structure containing silicon in octahedral coordination with hydroxyl and this octahedral group $[Si(OH)_6]^{2-}$ is stable up to approximately 110 °C [19]. There is a distinct peak at 658 cm^{-1} corresponding to Si–OH group in the Raman spectrum of thaumasite and the peak positions of gypsum are different from thaumasite and ettringite, making it easy to distinguish it from them. Thus, Raman spectroscopy is a valuable tool for positively identifying thaumasite in a mixture with ettringite and gypsum. Therefore, the presence of thaumasite, ettringite, gypsum and calcite are adequately demonstrated by the result in Fig. 8.

Table 2
Wave numbers of important infrared absorption bands

Wavenumber (cm^{-1})	Assignment, from [22]
3600–3200	H_2O stretch
1650	H_2O bend
1400	CO_3^{2-} stretch
1100	SO_4^{2-} stretch
940/920	SiO_4
887	CO_3^{2-} bend
850	AlO_6
673	SiO_6 stretch
590	SiO_4 bend
500	SiO_6 bend

4.4. FTIR spectrum

FTIR was carried out on the sample of deteriorated concrete and the infrared spectrum is shown in Fig. 9. The absorption bands present in the spectrum were identified by comparison with previously published data [20] shown in Table 2. Firstly, a peak was detected at 498 cm^{-1} which is assigned to the presence of SiO_6 bonds. Octahedral Si is such an extremely rare co-ordination state for mineral silicates that the presence of this peak must be indicative of either thaumasite or a thaumasite-containing solid solution [21].

Secondly, peaks at 875 cm^{-1} and 1385 cm^{-1} can be assigned to the C–O bending band and stretching band, respectively, and are attributable to the presence of the CO_3^{2-}. The peak at 1100 cm^{-1} associated with SO_4^{2-} is detected but there is no sign of AlO_6 at 850 cm^{-1}. The above again leads to the conclusion that the deteriorated concrete contains mainly thaumasite and little ettringite.

4.5. Discussion

The major contribution of this paper has been to determine whether the deterioration of the field concrete

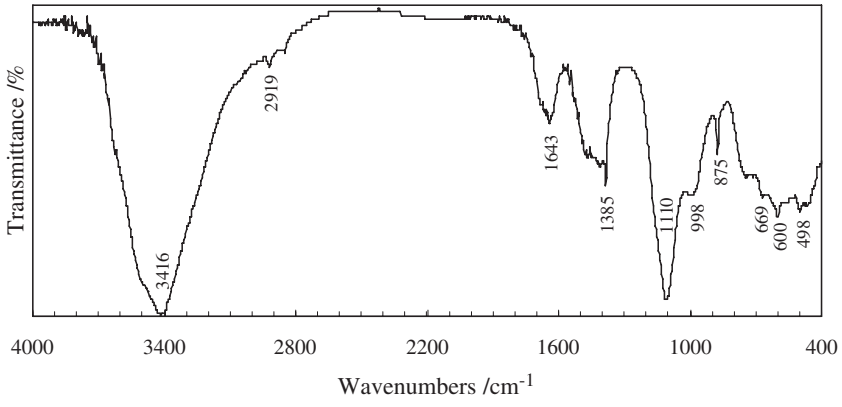

Fig. 9. FTIR spectrum of the deteriorated concrete.

was due to conventional sulfate attack associated with ettringite formation or to TSA. In fact, both thaumasite and/or ettringite were positively identified by XRD; needle-like crystals based on Ca, Si and S have been observed by SEM and analyzed by EDX; octahedral silicon (present in thaumasite but not in any other silicate phase likely to be formed from Portland cement) was detected by Raman and FTIR spectra. The evidence is, therefore, overwhelming that TSA is primarily responsible, together with ettringite formation, for the deterioration of the field concrete.

The mechanism of thaumasite formation in the field concrete has not yet been confirmed, but further works are in progress and will be published in future papers. Whilst the concrete deterioration occurred mainly in this tunnel, other portions of the dam were in sound condition. This may be due to the lower temperature and higher humidity inside the tunnel, both of which are favourable to TSA.

It was been found that the worst attack occurred on the concrete surface and deterioration decreased with depth from the surface, even if the groundwater containing sulfates penetrated into the tunnel in the opposite direction. This tends to suggest that the main source of carbonate exists at the concrete surface i.e. as a result of concrete carbonation.

In this particular dam, a low dose of cement with low C_3A was used, which limits the amount of ettringite that can be formed although a small amount of ettringite was observed (Fig. 5). In the specific field temperatures (<10 °C), calcium silicate hydrates (CSH) tend to react with sulfate, carbonate and water to form thaumasite [22] rather than ettringite and since thaumasite does not contain aluminium, the use of low C_3A cements are unlikely to provide any protection. At the same time, the classic form of sulfate attack and carbonation of concrete appear to have occurred and eventually the internal surface concrete of the tunnel has been decomposed into a white, non-binder, pulpy material, consisting of a mass of thaumasite crystals, together with crystals of ettringite, gypsum, calcite.

It can be seen that existence of CO_3^{2-} is an extremely important factor for TSA but that aluminium is the leading influence in the classic form of sulfate attack. This explains why concrete made with sulfate-resistant Portland cements (with low C_3A content) can suffer serious sulfate attack due to TSA. Thus, it has been demonstrated that TSA can play an important role in the deterioration of some concrete structures in Western China.

The data also shows that there is a very high concentration of Cl^- in the ground water. The detrimental role of Cl^- on TSA has been recently studied by Torres [23] who reported an increase in TSA in samples immersed in combined sulfate and chloride solutions at 5 °C. Friedel's Salt ($Ca_4[Al(OH)_6]_2Cl_2{\cdot}4H_2O$) was not observed among the attacked areas of the concrete which confirms Torres findings [23] that this mineral is unstable in the presence of chloride and carbonate ions in systems prone to develop thaumasite.

5. Summary

Thaumasite, as well as ettringite and gypsum, is a product of sulfate attack of concrete. The thaumasite form of sulfate attack (TSA) is now regarded as a primary cause of deterioration in many field structures in Western countries. There is hitherto no case of TSA reported in China, although sulfate attack of concrete involving the formation of ettringite and gypsum has been recognized and researched for many years. Thaumasite has similarities to ettringite in its crystalline structure, X-ray diffraction (XRD) pattern, microstructural features and many optical properties and therefore distinguishing between the minerals can be difficult. It is therefore likely that thaumasite may have been misidentified as ettringite in many deteriorated structures in the past.

This paper presents the first case of thaumasite-related sulfate attack of field structures in China. The XRD pattern, SEM–EDX analysis, Raman spectrum and FTIR spectrum demonstrate that the sulfate attacked paste was transformed into a white pulpy substance with no binding properties in which abundant thaumasite occurs together with some ettringite, gypsum and calcite. Spectroscopical methods (FTIR, Raman) are valuable in identifying thaumasite due to the existence of octahedrally coordinated silicon in its crystal structure.

Acknowledgments

This paper is supported by the Project 50378075 from the National Natural Science Foundation of China (NSFC).

References

[1] S.P. Varma, J. Bensted, Silicates Industriels 38 (2) (1973) 29.
[2] B. Erlin, D.C. Stark, Highway Research Record 115 (1965) 108.
[3] N. Crammond, Cement and Concrete Composites 24 (4) (2002) 393.
[4] N. Loudon, Cement and Concrete Composites 25 (8) (2003) 1051.
[5] Thaumasite Expert Group, The Thaumasite Form of Sulfate Attack: Risks, Diagnosis, Remedial Works and Guidance on New Construction, Department of the Environment, Transport and the Regions, London, 1999.
[6] M. Romer, L. Holzer, M. Pfiffner, Cement and Concrete Composites 25 (8) (2003) 1111.
[7] M. Romer, Cement and Concrete Composites 25 (8) (2003) 1173.
[8] S. Diamond, Cement and Concrete Composites 25 (8) (2003) 1161.
[9] G. Collett, N. Crammond, R.N. Swamy, et al., Cement and Concrete Research 34 (9) (2004) 1599.
[10] D.C. Stark, Cement and Concrete Composites 25 (8) (2003) 1119.
[11] T. Dijkstra, 20th WEDC Conference, Colombo, Sri Lanka, September 2004, From www.lboro.ac.uk/departments/cv/wedc/papers/20/dijkstra.htm.
[12] Y. Zhai, T. Cai, The Tertiary System of Gansu Province, People's Press of Gansu, 1984, p. 1, Translated by Will Down, Department of Geology, Bilby Research Centre, Northern Arizona University, April 1992.
[13] Z. Wang, Northwest Waterpower (Chinese) 2 (1994) 34.
[14] Building Research Establishment, Special digest 1: concrete in aggressive ground (SD1), Building Research Establishment, August, 2001.
[15] E.E. Lachowski, S.J. Barnett, D.E. Macphee, Cement and Concrete Composites 25 (8) (2003) 819.

[16] H. Yu, W. Sun, J.C. Wang, et al., Journal of The Chinese Ceramic Society (Chinese) 31 (5) (2003) 434.
[17] E.F. Irassar, V.L. Bonavetti, M. González, Cement and Concrete Research 33 (1) (2003) 31.
[18] S. Sahu, D.L. Exline, M.P. Nelson, Cement and Concrete Composites 24 (3) (2002) 347.
[19] A.R. Brough, A. Atkinson, Cement and Concrete Research 31 (3) (2001) 421.
[20] J. Bensted, S.P. Varma, Silicates Industriels 39 (1) (1974) 11.
[21] S.M. Torres, J.H. Sharp, R.N. Swamy, et al., Cement and Concrete Composites 25 (8) (2003) 947.
[22] J. Bensted, Cement and Concrete Composites 25 (8) (2003) 873.
[23] S.M. Torres, The influence of chloride on the thaumasite form of sulfate attack in mortar containing calcium carbonate, PhD Thesis, Faculty of Engineering, The University of Sheffield, August 2004.